LBC: the prime focus optical imagers at the LBT telescope

F. Pedichini[*a*], E. Giallongo[a], R. Ragazzoni[b], A. Di Paola[a], A. Fontana[a], R. Speziali[a] ,J. Farinato[b], A. Baruffolo[c], C. Magagna[c], E. Diolaiti[e], F. Pasian[d], R. Smareglia[d], E. Anaclerio[f], D. Gallieni[f], P. G. Lazzarini[f].

[a]INAF Oss. Astr. Roma; [b]INAF Oss. Astr. Arcetri; [c]INAF Oss. Astr. Padova, [d]INAF Oss. Astr. Trieste, [d]Astronomical dep. Padua University, [f]ADS International,

ABSTRACT

The Large Binocular Camera (LBC) is the double optical imager that will be installed at the prime foci of the Large Binocular Telescope (2x8.4 m) . Four italian observatories are cooperating in this project: Rome (CCD Camera), Arcetri-Padua (Optical Corrector) and Trieste (Software). LBC is composed by two separated large field (27 arcmin FOV) cameras, one optimized for the UBV bands and the second for the VRIZ bands. An optical corrector balances the aberrations induced by the fast (F#=1.14) parabolic primary mirror of LBT, assuring that the 80% of the PSF encircled energy falls inside one pixel for more of the 90% of the field. Each corrector uses six lenses with the first having a diameter of 80cm and the third with an aspherical surface. Two filter wheels allow the use of 8 filters. The two channels have similar optical designs satisfying the same requirements, but differ in the lens glasses: fused silica for the "blue" arm and BK7 for the "red" one. The two focal plane cameras use an array of four 4290 chips (4.5x2 K) provided by Marconi optimized for the maximum quantum efficiency (85%) in each channel. The sampling is 0.23 arcseconds/pixel. The arrays are cooled by LN2 cryostats assuring 24 hours of operation. Here we present a description of the project and its current status including a report about the Blue camera and its laboratory tests. This instrument is planned to be the first light instrument of LBT.

Keywords: Imager, CCD, optical corrector, wide field, LBT.

1. INTRODUCTION

The main architecture of the LBT (Fig. 3) telescope will be exploited by the LBC cameras: two mirrors will mean two different prime focus correctors one optimized for the UBV bands and another for the VRIZ bands working together for multi color imaging on the same sky area to acquire the maximum efficiency for multi wavelenght data. Of course the optical design for the Red channel differs from the Blue one mainly for the glass selection, here the BK7 replaces the Fused Silica. Also the CCD array uses a different technology (high resistivity thick silicon) to reach the high sensitivity requested in the red bands. For further details about the optomechanics of both channels see Diolaiti[14] et al. Spie 2002. The Blue camera will be the first light science instrument at the LBT telescope during summer 2004.

1.1 Optical design

The major difficulties in the design of a prime focus corrector for the LBT are represented by the focal ratio of the primary mirror (F/1.14), the large telescope diameter (8.4m) and the parabolic shape of the mirror. The blue channel design (Fig1.) can be described as a modification of the Wynne approach[1]. The latter consists of three lenses, basically correcting spherical aberration, coma and field curvature.

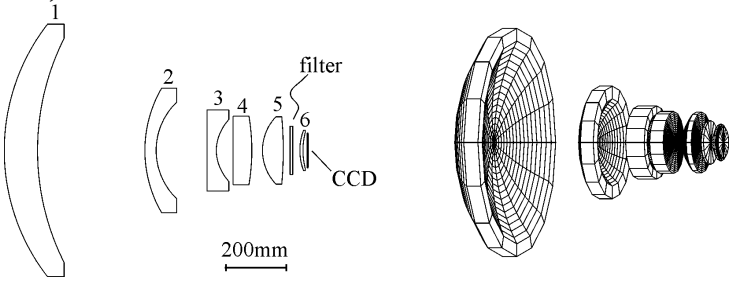

Figure. 1. Prime focus corrector optical design (2D layout and solid model)

[*] pedik@mporzio.astro.it ; pedik@tiscalinet.it ; phone +39 06 94286489; http://www.mporzio.astro.it ; INAF Oss. Astr. Roma Via Frascati 33, 00040 Monteporzio Catone ITALY

All the lenses are in fused silica, which ensures high throughput in the wavelength range of interest. The optical surfaces are spherical or plane, except lens 3 (L3) featuring an aspherical surface on the concave side. This surface is actually ellipsoidic and presents a departure from the best fit sphere of ≈700μm at the edge.

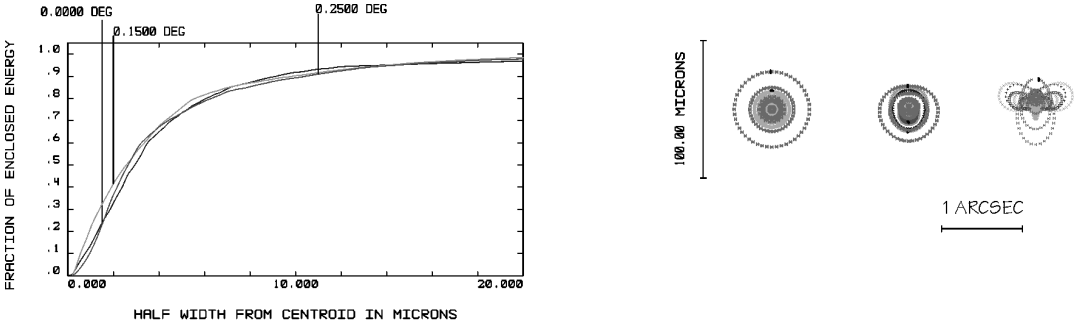

Figure 2. Optical performance of prime focus corrector. Left: polychromatic ensquared energy plot, showing the fraction of geometric energy ensquared in a box of given size, as a function of the box size itself. Right: polychromatic spot diagrams for different field angles (0°, 0.15°, 0.25°); the spot size is roughly 10 times larger than the Airy disk, indicating that the optics are not diffraction limited.

2. THE HUB MECHANIC

The mechanical design of the prime focus consists of two main parts: the hub that mounts the fixed lenses and the derotator which holds the filters wheels and the cryostat. Each one of the five fixed lenses is kineamtically mounted into an INVAR frame, which is then connected to the steel hub through flexure elements to accommodate the differential thermal expansion of the two materials. For the same reason, the two main lenses, which are 810 mm and 400 mm large, are mounted into their INVAR frames by means of special RTV pads, that are tailored to compensate for the differential thermal expansion of the glass and the INVAR.

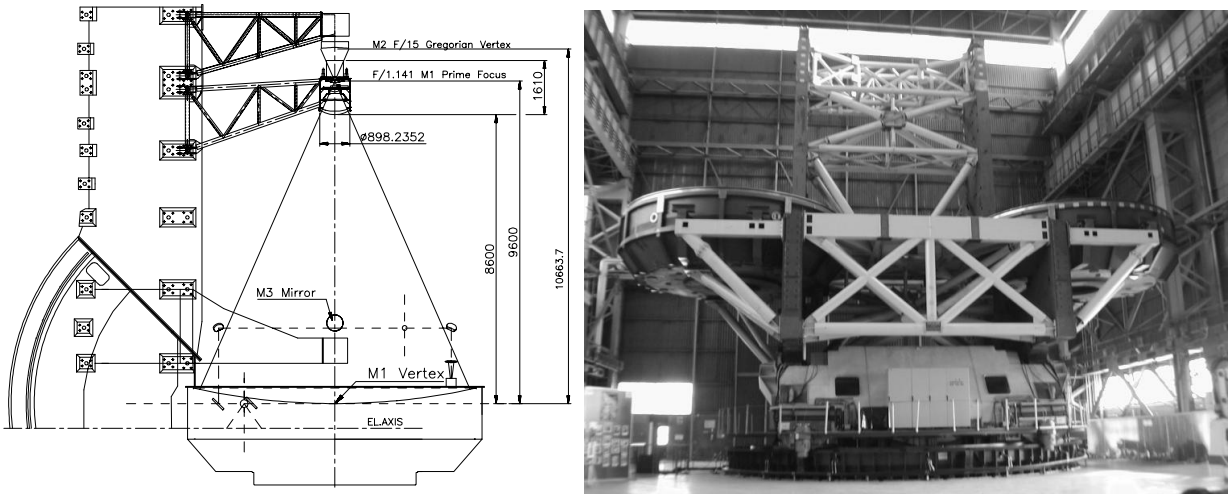

Fig. 3 Left: The LBC position within the LBT optical layout. Right: The LBT telescope in the workshop.

The derotator decouples the imager from the corrector lenses and hosts two filter wheels, the shutter and the cryostat. Each filter wheel is controlled through an anti-backlash gearing by a DC motor and an absolute encoder, again directly coupled to the wheel's gearing. Finally, the cryostat mount is suited to install all the instrument electronics on board the derotated structure. The mechanical design of the prime focus hub is shown in the following figure 4. The derotator module assure the control of the parallactic angle on the detector focal plane by means of a dual motor driving and an absolute encoder. The two 200 W brushless motors will work in closed loop, with the encoder, in push-pull to reduce any backlash of the system. The on axis resolution of 18 arcsec. will assure a sub pixel accuracy up to the edge of the

focal plane. The selected integrated PWM controller from Faulabher performs all the task needed for encoder readout and PID control of the motors leaving the control host computer free of any computation. Also the velocity profile of the derotation tracking is managed (once loaded by the host PC) by the controller itself. The control PC can, of course, get telemetry data (position, speed, power….) from the controller at any time, when or if requested, for checking or database pourposes. The same control philosophy as been applied to all the servo controls of the LBC instrument where each motor controller is addressed by the control PC as a network node by means of a TCP-IP protocol.

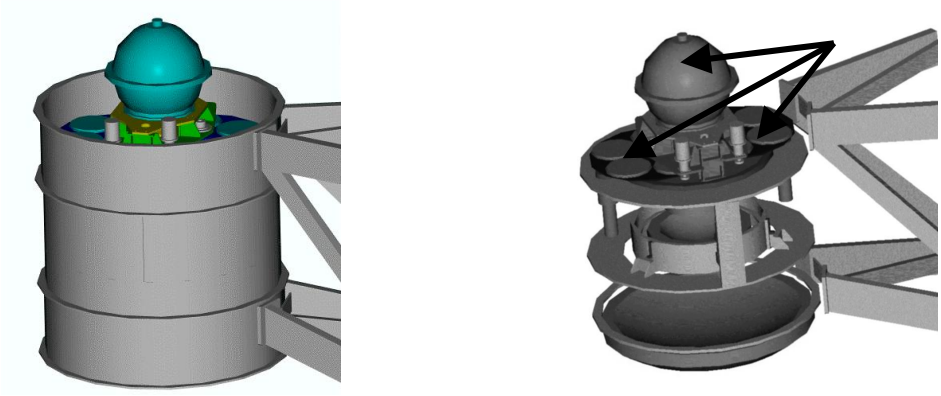

Fig. 4: Left: CAD wiev of the hub with the camera. Right: Cad view of the LBC's interiors where the arrows show the derotated components

3. CCD CAMERA

The cryostat was designed to cool down to 170*K* the detector flange that holds the scientific array composed by four MAT 42-90 chips and three more MAT detectors for technical use[2]. Our experience in making cryostats for CCD cameras (see Speziali[3] and Pedichini[4)] based on a LN_2 bath, led us to prefer this approach for LBC instead of other technologies used in similar instruments (Boulade[5], Mc. Leod[6]). The positive experience with the small camera built for the prime focus of the Schmidt telescope of Campo Imperatore guided us to design a cryostat composed by three independent modules: a stainless steel interface flange, a nitrogen vessel and a housing made of aluminium (see fig. 5). This configuration allows to separate the electrical part (detector flange, cables, etc) from the cryogenic assembly, allowing an easy maintenance and upgrade of the two parts independently.

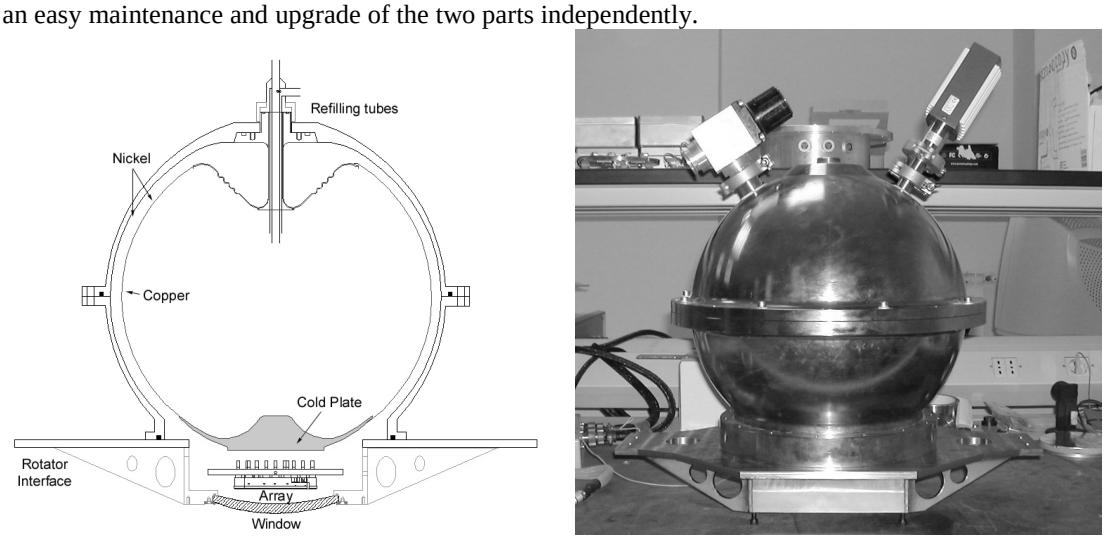

Fig. 5: The drawing and the picture of the cryostat with the three modules.

3.1 The vessel

The peculiar component of this cryostat, (Fig.5) by a mechanical point of view, is the bimetallic and monolithic vessel. It has been designed with a spherical shape both to minimize the radiative thermal inlet and to make a quite compact instrument. The vessel has been built by Forestal s.r.l. experiencing new mechanical technologies based on electroforming processes to produce the bimetallic sphere without any weldings. The inner part of the vessel is made by a copper sphere with a diameter of 320*mm* and a thickness of about 1*mm*. At the bottom of the sphere there is a copper

flange 100*mm* wide and 10*mm* thick representing the "cold plate" of the cryostat. With this geometry we should obtain both a smooth cooling of the CCD baseplate and a good temperature stability, being the latter independent of the position of the camera. A cilindrical cryogenic pump filled with zeolith is applied on the copper flange to keep the vacuum level between 10^{-4} and 10^{-5} *mbar*. On the opposite side of the cold plate we welded the refilling system based on stainless steel cryogenic tubes to minimize the thermal inlet by conduction.

3.2 The spherical case

The outer case (Fig.6) is aluminium made and consists of two halves of a sphere with a diameter 10*mm* larger than the vessel one and with a thickness of about 3*mm*. The two halves are covered by a 70-100 micron layer of Nickel to prevent the aluminium degassing and to ensure a high reflectivity of the inner surfaces after polishing. The two halves are joined by an O-ring. On the upper one we glued, using Torseal, two standard KF ISO flanges for pumping and vacuum sensors.

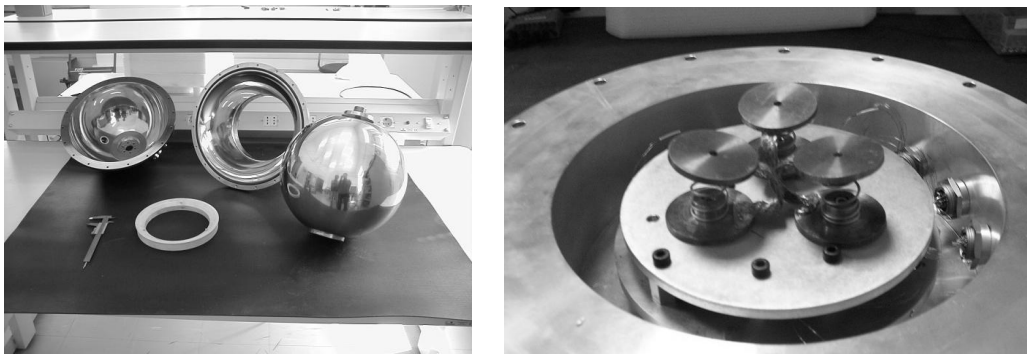

Fig. 6: Left: The cryostat dismounted. Right: The thermal links made up of three springs and copper pads

3.3 The derotator interface flange

This flange (see fig. 7 right) is made of a stainless steel (AISI 4130). It will hold the baseplate with the sensors and it interfaces the cryostat with the derotator of the prime focus. Ten Fischer vacuum connectors are used to connect the detectors to the outer read-out electronics. This interface was designed by us and the numerical simulation of the 3D model was carried on by ADS. As reported in figure 7 left the FEA analysis shows a very low deformation (2 μm) even with the telescope in the horizontal position.

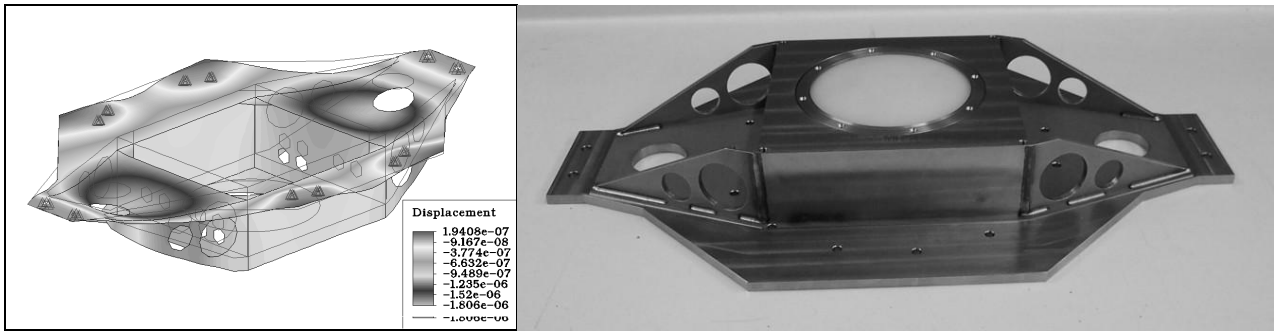

Fig.7. Left: FEA analysis of the flange. Right: The AISI 4130 flange with a dummy window.

3.4 Cooling the array

To cool the detectors we have developed a thermal link between the detectors flange and the vessel, fulfilling the following requirements:

- operative temperature of 170±2*K*;
- cooling speed below 5*K*/*min*, that is the maximum rate allowed by MAT;
- temperature stability of 3*K*;
- no active temperature control to avoid LN_2 extra consuming.

At the operative temperature of 170*K*, suggested by MAT, the best compromise between a low dark current (<1e/min) and a high quantum efficiency and charge transfer efficiency is achieved. Even a fluctuation of ±5*K* does not produce a

significant change in the performances. The sensor flange is stainless steel made and has been provided directly by MAT. It is attached to the dummy head of the cryostat by means of three fiberglass standings. On this flange 10 holes were provided to connect a second flange, made by aluminium, where the thermal links are mounted on. These links consist of three springs having two copper pads at the two ends (fig. 6 Right). The springs push the pads to the copper flange of the vessel when the cryostat is closed making a good thermal contact. Three copper wires were soldered connectings the two pads, and it is possible to adjust the operative temperature and, therefore, the cooling speed simply varying the diameter and the lengths of the copper wires. This system allows us to achieve a good temperature control and stability below 1K without any active heather.

3.5 Cryogenic tests

Several tests have been performed in the laboratory of the Rome Observatory between April 2001 and April 2002 to find the right sizes of the thermal link and the performance of the cryostat. In the last one (fig. 9) we simulated the movements of the camera of the telescope tilting the cryostat up to 60°.

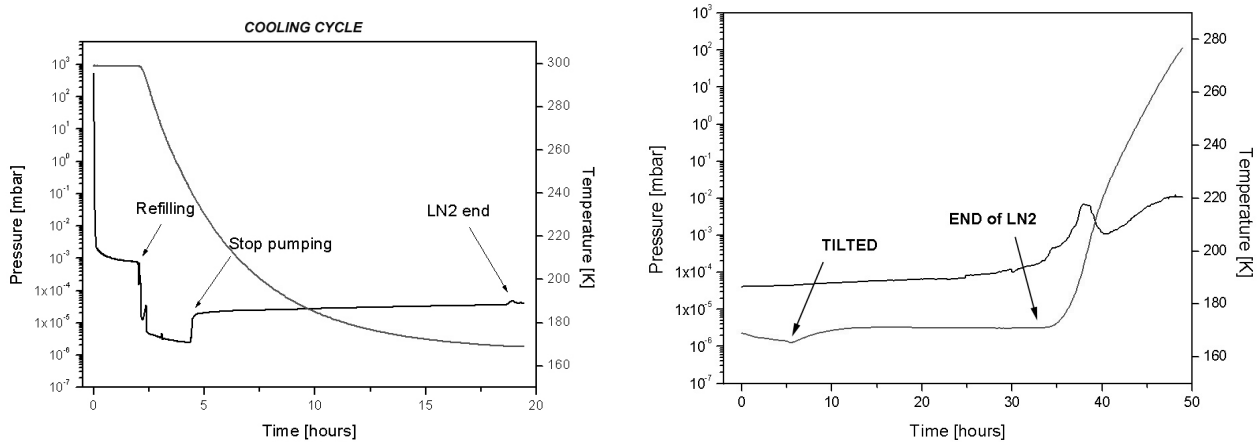

Fig 9.Left: Cooling test of the cryostat. Right:Temperature and pressure time plot after tilting the cryostat

As shown in figure 9 left, the operative temperature was 170*K*. After having reached this temperature the cryostat was refilled with about six liters of LN_2. Five hours later the temperature reached 168*K* and, after tilting the cryostat, the temperature reached 170*K* until the end of the cycle 30 hours later (fig.9 right). During the test the static vacuum changed from 4×10^{-5} to 8×10^{-5} being 1×10^{-2} after the complete heating. It took about 14 hours to reach the room temperature. From these test we have verified that the cryostat of the blue camera fulfills all the requirements of operative temperature and holding time. With this experience we are going to build the second one for the red channel making just a few changes. We will make the vessel by a single block of aluminium vessel using a CNC milling machine and we are developing, together with Forestal, a new process to weld the stainless steel refilling system to the aluminium vessel.

3.6 Focal plane ccd array

Three types MAT (*Marconi Applied Technologies*, ex EEV) detectors have been chosen to allow both the scientific data acquisition and the control of the intrument: an array of four MAT 42-90 (4.6K×2.5K) chips cover the corrected field (∅ = 27 *arcmin*) with a sampling of 0.23 arcsec/pixel providing the scientific image, while two MAT 42-10 will be used to acquire short exposure images for tracking and wavefront control. We are still evaluating the possibility to place another small chip, like the MAT06-02, for a real time low order aberration corrections.

3.7 The detectors placement

The four scientific MAT 42-90 chips are mounted on an invar plate as shown in fig. 10. This plate has been directly machined by MAT with the holes for the electrical connectors and for the orientation registers needed to align the detectors.

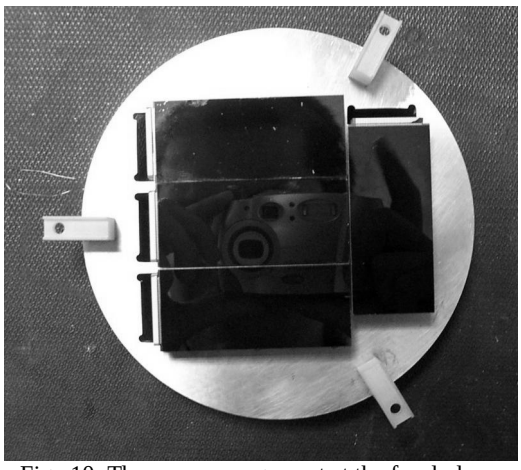

Fig. 10: The array arrangement at the focal plane.

The corrected fields have a diameter of 110*mm* and 108.2*mm* for the blue and red channel respectively and the four MAT42-90 chips cover about the 75% of these useful areas. As shown in figure 1 there is a 5% of energy loss, in the blue channel at the edge of the corrected field, while in the red channel this percentage of vignetting is well outside from the corrected area. The two MAT 42-10 chips will be placed at the two sides of the scientific array, mostly inside the corrected field and we are also investigating the opportunity to use also the small area near the fourth chip for installing a small MAT 06-02 chip for on-line wavefront analysis.

3.8 The MAT 42-90 detector

Two sets of four 42-90 grade-1 detectors were (Fig. 11) ordered following these requirements:

- QE > 85% at peak
- Charge Transfer Efficiency > 99.999%
- Read Out Noise < 5 electrons at 1MHz
- Dead Pixels < 1350
- Column Defects < 6
- Surface roughness < 7 μm peak to valley

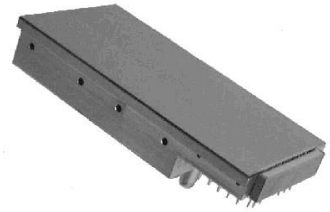

Fig. 11:The EEV 42-90 chip.

The last requirement is imposed by the very fast focal ratio of the camera ($F_{\#}$=1.41) and is needed to keep the nominal optical quality (80% of the energy in one pixel) of the image all over the focal plane. We have received all the eight 42-90 chips for both channels. The electrical and mechanical samples have been used to make the preliminary tests and set up of the blue channel camera. In the table 1 the QEs of the chips we have received are listed

CCD sn	350 nm	400 nm	500 nm	650 nm	900 nm	1000 nm
Blue channel array						
8341-16-3	53.8	81.3	85.4	78.8	28.3	-
8351-18-4	56.1	83.7	88.2	80.1	27.3	-
9283-4-5	53.8	81.1	83.8	76.8	27.4	-
9283-1-4	56.3	77.7	80.5	75.0	28.3	-
Red channel array						
9434-17-3	-	-	95.1	96.7	57.0	13.2
9434-16-5	-	-	82.8	90.2	53.2	11.8
9434-15-3	-	-	84.3	90.6	51.5	11.2
9434-15-4	-	-	87.4	95.7	54.4	12.2

Tab. 1: Quantum Efficiency of the scientific sensors.

3.9 The MAT 42-10 chips

This chip is a frame transfer CCDs. and will be used for guiding, realtime focusing and high order wavefront analysis. The refresh time of this system will be about 1Hz. We performed a simulation of the images given by the 42-10 chips (fig.11 left) to evaluate the sampling time needed to track a field star. Conservatively, we considered 1 *arcsec* of seeing,

and we requested a centroid determination accuracy better than 0.02 *arcsec*. Because of the position of the trackers on the same focal plane of the science array, the attenuations and bandwidths of the science filters have been considered. Taking into account the CCD Q.E. response we ran the simulation using stars with a magnitude range from 15 to 20 and the results are exposure times always below 2-3 seconds. The total sky coverage of the 2 trackers is about 4.5 squared *arcmin.* Therefore combining the chip performance, the area and the number of star in one squared degree following the Bahcall model, we expect to find at least one reference star with $M_V = 19$ or $M_B = 20$ at high galactic latitude.In the U band, due to the low surface density of bright stars , we may consider to slightly modify the pointing by changing the paraxial angle when a fast tracking loop using a bright (Mag.U <18) star will be needed.

3.10 The Wavefront analysis

Two wavefront analysis modes are planned for the LBC to best exploit the funcionalities of the active primary mirror of LBT. A real time wavefront analysis acquiring a defocused PSF at the edge of the field by means of a CCD MAT 02-06 (380 x 280 pixels) installed about 0.2 - 0.3 *mm* below the optical focal plane. We espect with this mall chip to detect always, with an integration time less than 20-30 sec, a defocused star bright enough to be recorded with a good S/N for the computation of the low order aberrations (tip-tilt, defocus, coma, astigmatism). An *off line* analysis will be performed using a peculiar beam splitter (fig. 11 right) applied to the edge of the MAT 42-10 trackers. In this case when a star is centered on its face, two images of the source are produced on the CCD giving an extrafocal and an intrafocal PSF of the same star. Both PSF will cover several pixels yielding the opportunity to extract the high order aberrations for a primary mirror fine tuning. The expected loop time is about 15 sec. with a 15 or 16 Mag. star.

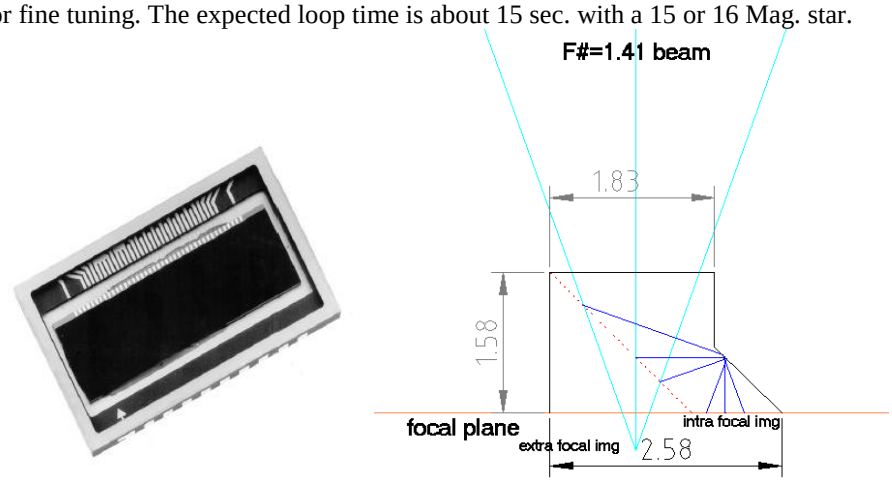

Fig. 11: Left: the MAT 42-10 chip. Right: The beam splitter for the high orders WF analysis

3.11 CCD controller

The CCD controller selected for the LBC camera is produced by the italian firm Elettromare and has been developed with the contribution of the italian astronomical community. Indeed it is an evolution of the standard CCD controller for the instrumentation of the National Galileo TNG telescope in La Palma Canarian. The main feature of this system is constituted by the absence of any microprocessor and intelligence inside the camera head. The whole system is composed by three boards. A PCI interface board, that hosts a DSP MOTOROLA 56301, provides all the clocks and control signals by means of a high speed fiber link (1.2 Gbit/s) transferring in real time all the data patterns to a re-syncronizing and parallelizing gate array placed on the SEQUENCER BOARD in the camera head. An ANALOG BOARD provides 8 programmable biases and acquires four video channels. This architecture allows a reduced heat dissipation in the camera head electronics and a very compact housing can be built around the three boards (VME format) needed to drive the chip array. The incoming data rate is 4Mpixel/s and WIN NT – WIN 2000 driver has been developed to store the data in the control PC memory. Standard aux. digital and analog I/O are provided in the camera head to perform system telemetry and the read-out of temperatures, voltages, vacuum levels and logic lines. Two dedicated output lines are provided to drive a standard iris shutter with its holding current and a small heather to lock the temperature of the CCD array with a 12 bit resolution via a simple P.I.D. filter. A general description of the architecture and philosophy of this system can be found in Bonanno[9]. The actual performances are a readout time of less than 15 sec. for the full array and a RON of about 10-12 e-. The final version of the CCD controller to be installed at the prime focus spider will have a different boards layout to be hosted in a small housing due to a large use of VLSI gate arrays to better comply with the weight and dimensional constraints of the LBC cameras and will be assembled as table

2 where can be compared to the laboratory controller. A reduced version of this controller with 2 only video channel will be used to drive the technical chips for tracking and WF sensing.

Card size	*Supply*	*Data Link*	*Video channels*	*Control lines*	*Programs*
3 Eurocard	Int. Power Supply	G-link to host	4 Video Ch.@1Mpix/s	16 Clok-16 Bias	Full
3-2 ½ Eurocard	Ext. Power supply	G-link to host	4-2VideoCh.@1Mpix/s	10 Clock-16 Bias	Reduced

Table.2 CCD Controller comparison for the LBC (first line laboratory actual controller second line compact controller).

3.12 Shutter

Three main constraints drow the project of the shutter (fig.12) for this camera they are: 1) A wide unvignetted shutterable aperture greater than 12 x 12 cm.; 2) Maximum tickhness of 17 mm. and less of 8 mm. in the central part; 3) Exposure uniformity on the whole field better than 1/100 mag. at 1 sec. exposure time. Secondary constraints were the need for a RS 232 control interface to easy program all the shutter control electronics, to readout the "real exposed time" and to perform an automated test procedure. Item #3 can be easily satisfied by means of a dual blades (or slit) shutter system similar to those used on 35 mm Reflex cameras. Following this approach we evolved the shutter realized in collaboration with CFR of Padova Italy (Pedichini[7]) for the TNG imager and for the SUSI 2 imager of ESO (D'Odorico[8]), but items #1 and #2 forced this project the use rigid CFK or aluminum blades instead of thin rollable steel blades cables pulled.

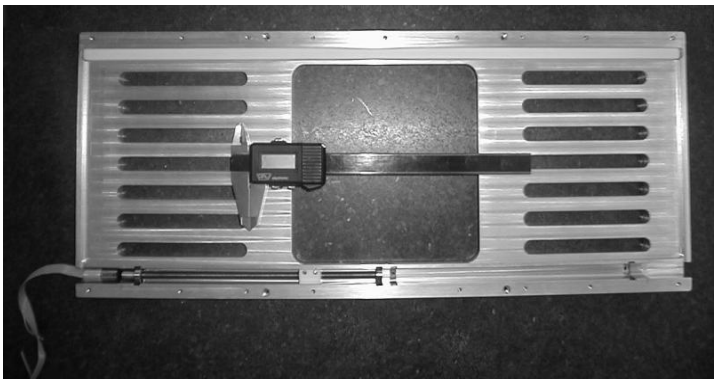

fig.12. Shutter frame top wiev with one motor installed.

The rigid blade are operated by constant speed electric motors via a nut-wormgear screw mechanic and slide on teflon side rails. To allow a closed loop control of the blades motion we have selected the Faulhaber D.C. motor model 1524E012SR equipped with a 128 step/turn digital magnetic micro-encoder. The diameter of this motor with its encoder is only 12 mm. and the "magnetic" Hall effect encoder removes the problems due to the unavoidable stray light always present in miniaturized "optical" encoders (fig.13 left). The use of 2 Hall sensors attached to the metal body and small Nd magnets glued to the blades allows the homing of each blade. The selected integrated micro controller manages the two axes (blades) by means of an integrated CPU performing a P.I.D. algorithm with a 5 Khz sampling time and furnishes the requested serial port RS232 to interface the shutter to the control network of the camera. Auxilary digital input and output pins on this motion controller allow a direct control of the shutter trough the CCD controller digital parallel port. The main body of this shutter is 14 mm thick (fig.12), and has been milled from Avional with CNC machining and electrolythic erosion to furnish smooth surfaces for the two blades rails. These rails host a Teflon border to protect them from oxidation and to reduce friction (fig 13 right). The time for a complete opening of the shutter is about 2 sec. but shorter exposures can be realized triggering the travel of the second blade few msec. after the first. The control CPU nulls the reload time alternating the working cycle between the exposures. Optical tests of the first prototype show an exposition accuracy of 0.56 msec. RMS at an exposure time of 460 msec. well below the maximum error accepted of 4.6 msec. RMS.

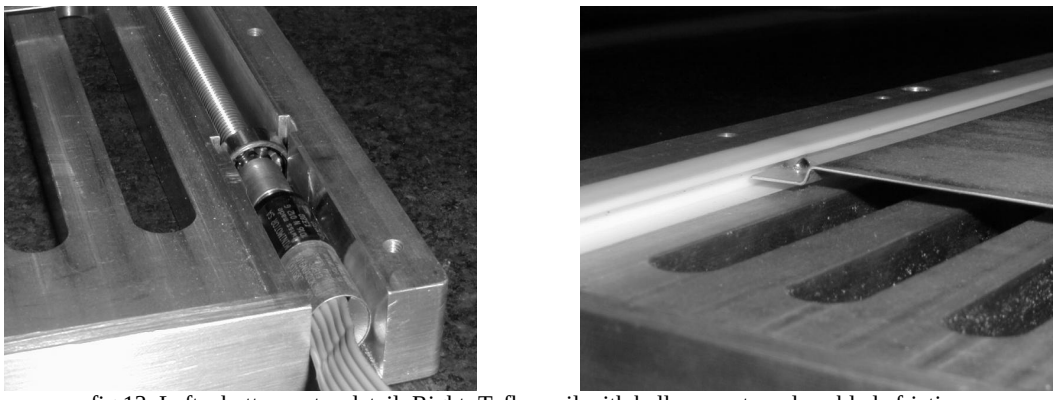

fig.13. Left: shutter motor detail. Right: Teflon rail with ball cursor to reduce blade friction

4. LBC SOFTWARE

4.1 Low level control

The structure of the low level control software for the LBC cameras depends essentially on the requirements of the various hardware components. A PC called Central Management Unit (CMU) receives from the User Interface program (UI) an Observing Block (OB) describing an observational sequence. The OBs are usually prepared by the observer in advance and handle both simple observations like "Acquire an image in the R band" or more complex tasks like "Acquire a set of 10 images in the V,R and I filters of 600, 450 and 300 sec. each, offsetting the telescope by 20" between each". As soon as the CMU receives an OB, it asks the night assistant for an execution confirmation and then provides structure unpacking, operations scheduling and devices control up to the final images production. Each LBC camera is composed by many devices, from the control software point of view there are 8 serial lines, 4 Profibus and 2 CCD controllers for each camera. Some devices requiring only non real-time controls are directly driven by the CMU, other that instead involve more time critical operations are controlled by dedicated PCs. Typical time critical operations requiring a dedicated PC are those regarding CCD readout. Each of these machines runs the Windows 2000 operating system and is equipped with a dedicated PCI interface board to communicate with the CCD controller electronics. The Linux driven CMU PC talks to each CCD PC through TCP sockets to command actions and retrieve system status. About acquired images, those coming from the scientific devices are compiled in a complete FITS file directly by the acquisition PC and then moved to an NFS shared area where they are available to the users and the archive routines, the images coming from the technical chips instead are processed and archive on board the acquisition PC and only products (stellar barycenters for star trackers or wavefront description for Active Optics) are returned to the CMU. The CMU is the only machine allowed to communicate with the telescope system both for pointing requests and for status reports queries.

4.2 Wavefront analysis

The Image Analysis (IA) subsystem of the LBC Control Software is in charge of computing the image quality in the focal plane, starting from defocussed star images acquired with auxiliary detectors, and to pass computed aberration coefficients to the telescope control software for active optics correction computation and application. One auxiliary CCD in the LBC focal plane (see Figure X) is dedicated to IA only (hereafter IA-CCD), while two additional auxiliary CCDs are devoted both to IA and autoguiding (hereafter AG-CCDs). The IA-CCD is used to compute aberrations during the execution of scientific exposures. An optical system, placed in front of it, slightly shifts the focal position so that an out-of-focus image will fall on the IA-CCD for each star in the Field of View (FoV). On the other hand the AG-CCDs are used for IA purposes only after pointing and before the beginning of the observations. An optical system covers an area of the AG-CCDs dedicated to IA and splits the light beam to produce an intra-focal and an extra-focal image of one star. After each preset, the telescope is offset so that one star, suitable for IA, falls on one of the AG-CCDs. After that an exposure is taken by the instrument control software (ICS) with the AG-CCD and delivered to the IA software for the computation of the aberrations that are then returned back to ICS. ICS then forwards them to the telescope control system for correction computation and application. This procedure can be repeated until a given convergence criterion is met. After the initial corrections have been applied, the telescope can then be offset back to the target in order to begin observations. From this point on IA is performed using the out of focus images taken with the IA-CCD. The algorithm for the computation of the aberrations is similar for the images acquired with the IA-CCD and the AG-CCDs: the underlying principle is that of curvature sensing (Roddier[10]). The algorithm for wavefront

reconstruction from its laplacian, computed starting with images from the AG-CCDs, is taken from Roddier & Roddier[11]. For single out-of-focus images acquired with the IA-CCD the wavefront is reconstructed following the method proposed by Hickson[12,13]. The Image Analysis software is meant to be a subsystem of the LBC ICS and interfaces with ICS only. Aberrations computation is triggered by the reception from ICS of one image acquired with the IA-CCD or AG-CCD. Results of the IA computations, plus a few status information, are then passed back to ICS, that takes care of delivering them to the telescope control software (TCS). TCS will then decide autonomously wether to apply the corrections or not and will eventually compute the forces to apply to M1.

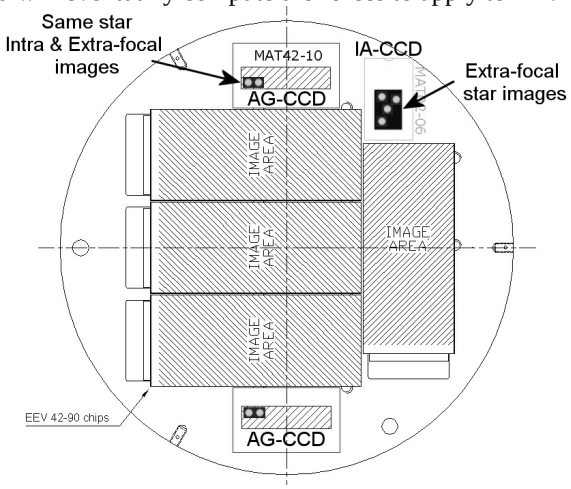

Fig.X .Location of the auxiliary CCDs used for autoguiding (AG-CCD) and image analysis (IA-CCD) in the LBC focal plane. Only part of the sensistive surface of the AG-CCDs is used for wavefront sensing, while the IA-CCD is entirely devoted to image analysis.

4.3 User interface

The LBC instrument will be operated through a Graphical User Interface (GUI) that will allow the user to define the planned observations, The key concept used in the following is the Observing Block (OB), intended as a set of observations that are conceptually similar and linked, and that share the same main pointing for the telescope. The GUI will allow the user to define the instructions for the execution of each OB. Although the GUI will definitely run at the telescope site, a portable version is foreseen for remote use. The application will be written in Java to be machine-independent. The GUI will store the content of each OB on individual files, in a simple ASCII-XML format to be processed by the Central Management Unit. The GUI will use menus and wizards to allow the insertion of the observing parameters required for each of the two imaging cameras and the metadata useful to describe the kind of data acquired (exposure type [science,calibration,ing_mode], observer name, program name, instructions to the pipeline, etc.) In the fully binocular operational mode, some of these parameters can be constrained on one of the cameras (the "slave" one) to prevent damage or loss of data on the other ("master"). Where appropriate, the GUI will also offer the option of recomputing some observational parameter to reach some user-defined goal. A typical case will be the scaling of the exposure time to reach a predefined S/N under varying seein or airmass conditions. The figure 12 show the design of the module for Interactive Pointing and the window used to ingest the main parameters.

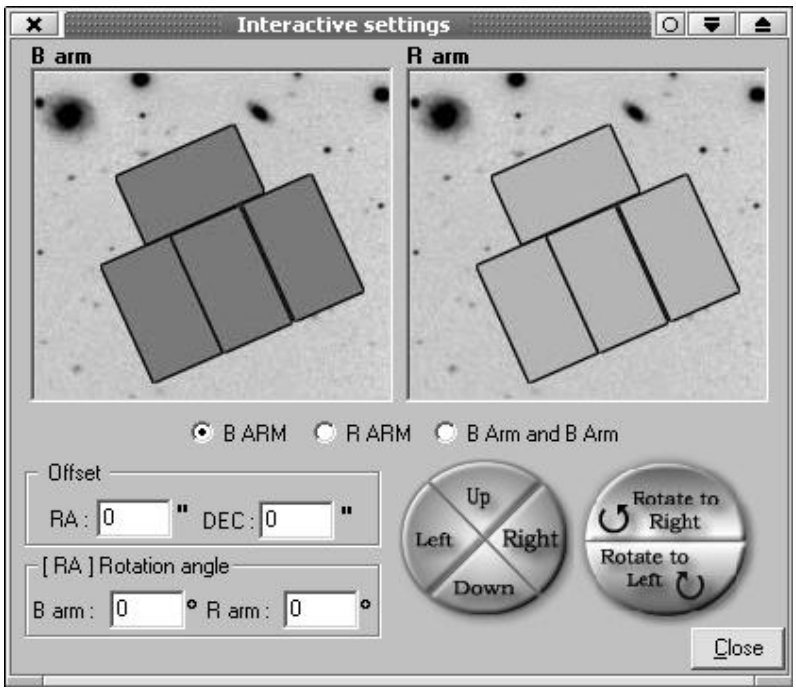

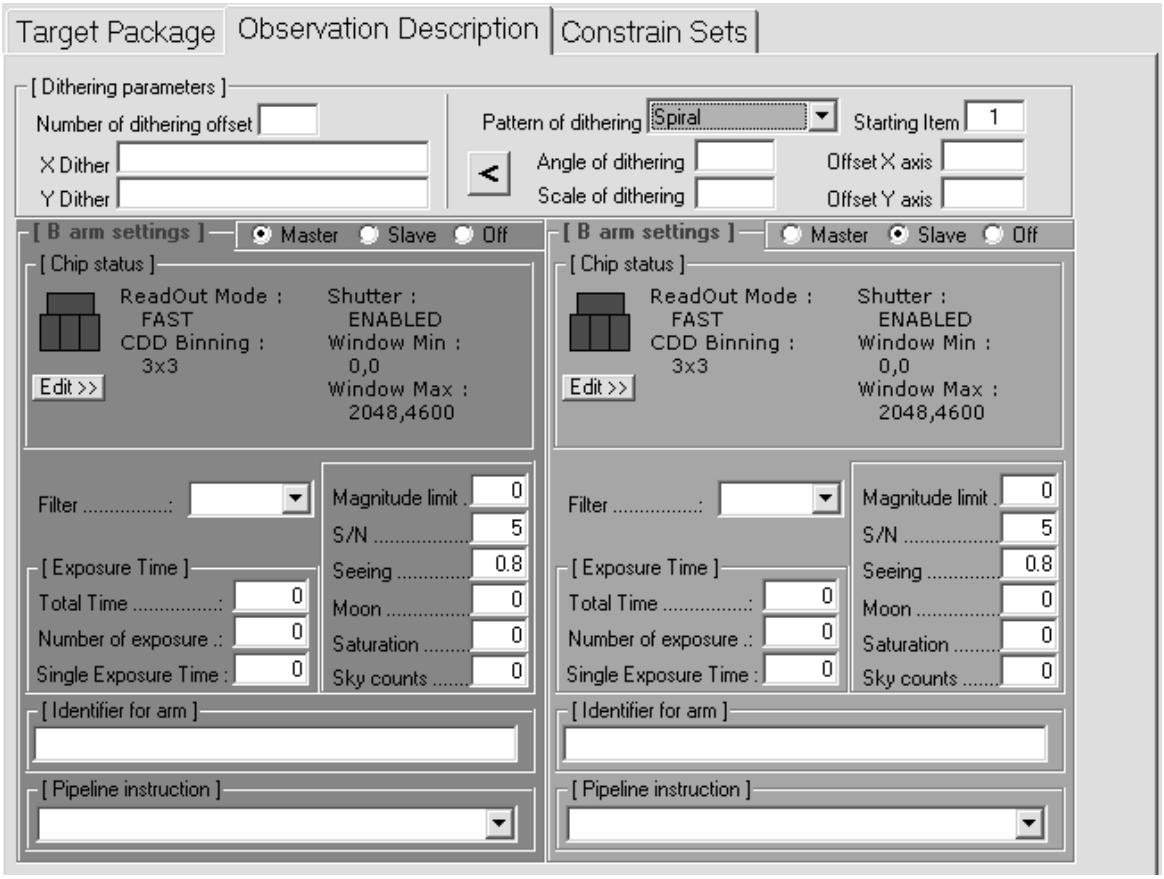

Figure 12. User interface menus at the MCU computer for OB compiling.

5. REFERENCES

1. R. Ragazzoni, E. Giallongo et al., "Double Prime focus camera for the F/1.14 large binocular telescope", 2000 - Proc. SPIE 4008, pp. 439-446.
2. Pedichini F., Speziali R. Proc. SDW 2002 conference Kluver Academic Publishers - J.W. Beletic & P. Amico eds. Hawaii June 2002 ..in press.
3. R. Speziali, F. Pedichini, "Design of a new cryostat for the Schmidt Telescope at Campo Imperatore", , 1997 - Internal Report, OAR/97/IR 2.
4. F. Pedichini, R. Speziali, F. D'Alessio, A. Di Paola, "ROSI: a compact 2kx2k CCD imager for the Schmidt telescope", 2000 - Proc. SPIE 4008, pp. 389-396.
5. O. Baulade, et al., "Development of MegaCam, the next generation wide field imaging camera for the 3.6m Canada-France-Hawaii Telescope", 2000 - Proc. SPIE 4008, pp. 657-668.
6. B. A. McLeod, M. Conroy, T. M. Gauron, J. C. Geary and M. P. Ordway: "MegaCam: paving the focal plane of the MMT with silicon", 1998 - Proc SPIE 3355, pp. 447-486.
7. Pedichini F., Comari M., Cosentino R., Farisato G., De Baco W., Sandre G. - High precision shutter for the TNG CCD Camera. Optical detectors for Astronomy - Kluver Academic Publishers - J.W. Beletic & P. Amico eds. (1998).
8. D'Odorico S., Beletic J.W., Amico P., Hook I., Marconi G., Pedichini F., - Commissioning of a 4Kx4K CCD mosaic and the new ESO FIERA CCD controller at the SUSI-2 imager of the NTT, Proceedings SPIE, vol. 3355, pag 507 (1998).
9. Bonanno et al., TNG new generation CCD controller. Optical detectors for Astronomy II- Kluver Academic Publishers - J.W. Beletic & P. Amico eds. (2000).
10. F. Roddier, "Curvature sensing and compensation: a new concept in adaptive optics," Appl. Opt. 27, pp. 1223-1225, 1988.
11. F. Roddier and C. Roddier, "Wavefront reconstruction using iterative Fourier transform," Appl. Opt. 30, pp. 1325-1327, 1991.
12. P. Hickson, "Wave-front curvature sensing from a single defocused image," JOSA A 11, pp. 1667-1673, 1994.
13. P. Hickson and G. Burley, "Single-image wavefront curvature sensing," Proc. SPIE 2201, pp. 549-554, 1994.
14. Diolaiti et al., "Blue and Red channel of LBC: a status report on the optics and mechanics", *this conference.*